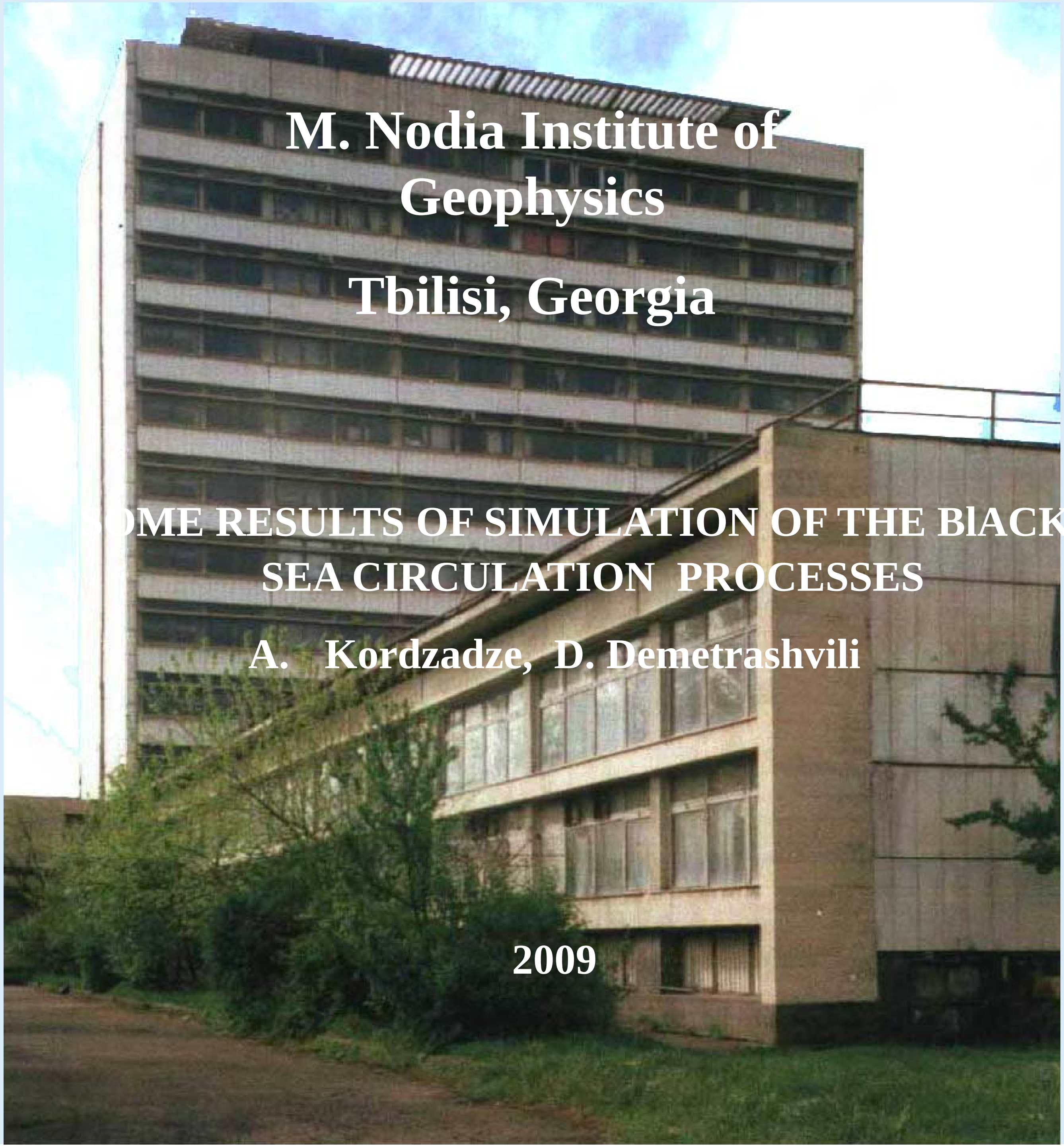

M. Nodia Institute of Geophysics

Tbilisi, Georgia

SOME RESULTS OF SIMULATION OF THE BlACK SEA CIRCULATION PROCESSES

A. Kordzadze, D. Demetrashvili

2009

The main goal of the Georgian team on mathematical modeling is to develop the Black Sea modeling system which will enable us to forecast hydrophysical fields for the Georgian Black Sea coastal zone with high resolution. This regional modeling system must be one of the components of the Black Sea nowcasting/forecasting system, which includes weather forecast model, basin-scale model of the Black Sea dynamics, satellite system and some regional models with high resolution. We have been cooperating for a long time with MHI(Sevastopol/Ukraine) in this area. The result of this cooperation was our participation in the pilot experiment performed in 2005 within the Intern. Project **ARENA** funded by EU. The prognostic calculations of the main hydrophysical fields (currents, temperature, salinity) with 1km spacing in some part of the Georgian Black Sea coastal zone in the near-real time regime was a part of the pilot experiment. With this purpose our 3-D baroclinic prognostic model of the Black Sea dynamics was adapted to some part of the Georgian Black Sea coastal zone (the liquid boundary was passing along meridian 41E) and was nested in a basin scale model of MHI(Fig.1).

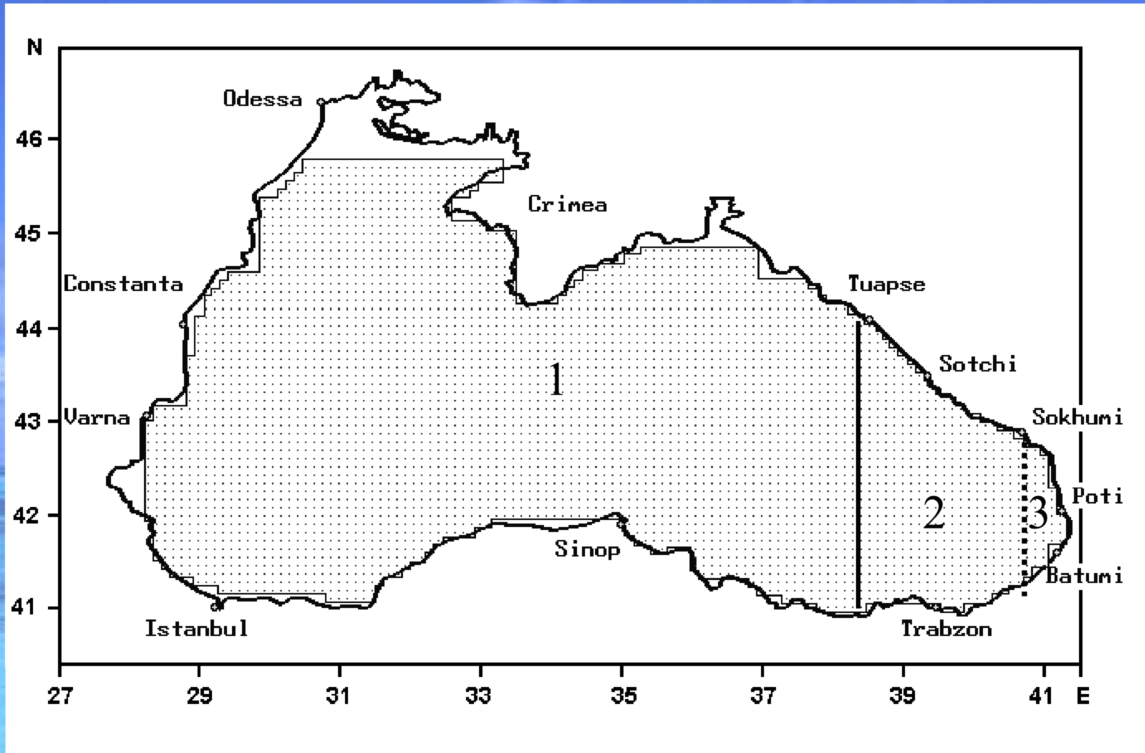

Fig.1. The model domains

At present, we are preparing a new version of the regional model, where the liquid boundary coincides with the meridian passing near the Tuapse city. We are expected to get necessary input data for our nested model from MHI with the purpose of adapting our model to the basin scale model of MHI, but there are some temporal technical difficulties in receiving these data via internet, and we hope in the nearest future we will have got all necessary input data. Before this we perform works to adapt the new version of the regional model to our `BSM.

We will present some results of modeling of the Black Sea circulation, which we have carried out recently with the use of our Black Sea dynamics models.

BAROCLINIC PROGNOSTIC MODELS OF THE BLACK SEA DYNAMICS

Basin-scale model → High resolution nested grid regional model

The models take into account:

- Atmospheric wind and thermohaline forcing;
- Sea bottom topography;
- Absorption of short-wave radiation by the sea upper mixed layer;
- Space-temporal variability of horizontal and vertical turbulent exchange;
- Water exchange with the Mediterranean Sea (for the basin-scale model);
- Danube River inflow (for the basin-scale model).

The models are based on a full system of ocean hydro-thermodynamic equations in z coordinates and represent improvement of the prognostic model of sea dynamics developed for the first time for the Black Sea in the 1970s in the Computing Center of Siberian Branch of the Academy of Sciences of USSR (Novosibirsk-Akademgorodok; *Kordzadze, Skiba 1973; Marchuk, Kordzadze, Skiba 1975; Marchuk, Kordzadze Salesny 1979; Marchuk, Kordzadze 1986; Kordzadze 1988).*

1. The model equation system

$$\frac{\partial u}{\partial t}+\mathrm{div}\vec{u}u-lv+\frac{1}{\rho_0}\frac{\partial p'}{\partial x}=\nabla\mu\nabla u+\frac{\partial}{\partial z}\nu\frac{\partial u}{\partial z},$$

$$\frac{\partial v}{\partial t}+\mathrm{div}\vec{u}v+lu+\frac{1}{\rho_0}\frac{\partial p'}{\partial y}=\nabla\mu\nabla v+\frac{\partial}{\partial z}\nu\frac{\partial v}{\partial z},$$

$$\frac{\partial p'}{\partial z}=g\rho', \qquad \mathrm{div}\,\vec{u}=0,$$

$$\frac{\partial T'}{\partial t}+\mathrm{div}\,\vec{u}T'+\gamma_T w=\nabla\mu_T\nabla T'+\frac{\partial}{\partial z}\nu_T\frac{\partial T'}{\partial z}+\frac{\partial\nu_T\gamma_T}{\partial z}-\frac{1}{c\rho_0}\frac{\partial I}{\partial z}-\frac{\partial\overline{T}}{\partial t},$$

$$\frac{\partial S'}{\partial t}+\mathrm{div}\,\vec{u}S'+\gamma_S w=\nabla\mu_S\nabla S'+\frac{\partial}{\partial z}\nu_S\frac{\partial S'}{\partial z}+\frac{\partial\nu_S\gamma_S}{\partial z}-\frac{\partial\overline{S}}{\partial t},$$

$$\rho'=\alpha_T T'+\alpha_S S', \quad \gamma_T=\frac{\partial\overline{T}}{\partial z}, \quad \gamma_S=\frac{\partial\overline{S}}{\partial z}, \quad \nabla\mu\nabla=\frac{\partial}{\partial x}\mu\frac{\partial}{\partial x}+\frac{\partial}{\partial y}\mu\frac{\partial}{\partial y},$$

$$T=\overline{T}(z,t)+T'(x,y,z,t),\ S=\overline{S}(z,t)+S'(x,y,z,t),\ \rho=\overline{\rho}(z,t)+\rho'(x,y,z,t),\ p=\overline{p}(z,t)+p'(x,y,z,t),$$

$$I=R_O e^{-\alpha z}, \quad R_0=\eta(1-A)I_0, \quad \eta=1-(\tilde{a}+\tilde{b}\tilde{n})\tilde{n},$$

$$I_0=a\sinh_\Theta-b\sqrt{\sinh_\Theta}, \quad \sinh_\Theta=\sin\varphi\sin\psi+\cos\varphi\cos\psi\cos\frac{\pi}{12}t,$$

$$\alpha_T=\partial f/\partial\overline{T}=-10^{-3}(0.0035+0.00938\overline{T}+0.0025\overline{S}),$$

$$\alpha_S=\partial f/\partial\overline{S}=10^{-3}.(0.802-0.002\overline{T}).$$

This equation system is written for deviations of thermodynamic values from their standard vertical distributions.

Designations:

u, v, w – the components of the current velocity along axes x, y, z, respectively;

T', S', P', ρ' - deviations of temperature, salinity, pressure and density from their standard vertical distributions $\overline{T}, \overline{S}, \overline{P}, \overline{\rho}$;

$l = l_0 + \beta . y$ - the Coriolis parameter;

g, c, ρ_0 - the gravitational acceleration, the specific heat capacity and the average density of seawater;

$\mu, \mu_{T,S}, \nu, \nu_{T,S}$ - the horizontal and vertical eddy viscosity, heat and salt diffusion coefficients, respectively;

I_0 - the total radiation flux at $z = 0$;

$A, h_{\Theta}, \varphi, \Psi$, - albedo of a sea surface, the zenithal angle of the Sun; the geographical latitude, the parameter of declination of the Sun;

$a, b, \tilde{a}, \tilde{b}$ - the empirical factors;

α - the parameter of absorption of short-wave radiation by seawater;

2. Boundary and initial conditions

at the sea surface $z = 0$

$$\frac{\partial u}{\partial z} = -\frac{\tau_{zx}}{\rho_0 \nu}, \qquad \frac{\partial v}{\partial z} = -\frac{\tau_{zy}}{\rho_0 \nu},$$

$$T' = T^* - \overline{T}(0,t) \quad \text{or} \quad \nu \frac{\partial T}{\partial z} = Q^T - R_0; \qquad S' = S^* - \overline{S}(0,t) \quad \text{or} \quad \nu \frac{\partial S}{\partial z} = (PR - EV) S_0;$$

at the sea bottom $z = H(x, y)$

$$u = 0, \; v = 0, \; w = 0, \; \partial T'/\partial z = -\gamma_T, \; \partial S'/\partial z = -\gamma_S;$$

on the lateral surfaces

$$u = 0, \; v = 0, \; \partial T'/\partial n = 0, \; \partial S'/\partial n = 0 \qquad \text{on} \quad \Gamma_0,$$

$$u = \tilde{u}, \; v = \tilde{v}, \; T' = \tilde{T}', \; S' = \tilde{S}' \qquad \text{on} \quad \Gamma_1.$$

at $t = 0$

$$u = u^0, \; v = v^0, \; T' = T'^0, \; S' = S'^0.$$

$\tau_{zx}, \tau_{zy}, T^*, S^*$ - wind stress components, temperature and salinity on a sea surface $z = 0$, respectively;

Γ_0 and Γ_1 – the rigid and liquid lateral boundaries;

$\tilde{u}, \tilde{v}, \tilde{T}', \tilde{S}'$ - the velocity components, deviations of temperature and salinity on liquid boundary, respectively;

$Q^T(x, y, t)$, $PR(x,y,t)$ and $EV(x,y,t)$ - The total heat flux, precipitation and evaporation on the sea surface.

The model enables to take into account atmospheric forcing by using Dirichlet conditions on a sea surface for temperature and salinity or Neumann conditions by given of heat fluxes, evaporation and atmospheric precipitation.

3. Calculation of turbulent field

Factor of horizontal turbulent viscosity was calculated by the formula offered by Zilitinkevich and Monin (1971)

$$\mu = \Delta x.\Delta y \sqrt{2\left(\frac{\partial u}{\partial x}\right)^2 + \left(\frac{\partial u}{\partial y} + \frac{\partial v}{\partial x}\right)^2 + 2\left(\frac{\partial v}{\partial y}\right)^2}, \quad \mu_T = \mu / c_T \qquad \mu_S = \mu / c_S .$$

Factors of vertical diffusion for heat and salt were calculated by the formula offered by Marchuk, Kochergin et al (1980)

$$\nu_{T,S} = (0.05h)^2 \sqrt{\left(\frac{\partial u}{\partial z}\right)^2 + \left(\frac{\partial v}{\partial z}\right)^2 - \frac{g}{\rho_0}\frac{\partial \rho}{\partial z}},$$

h - the thickness of a turbulent surface layer which is defined by the first calculated point z_m, in which the following condition is satisfied:

$$(0.05z_m)^2 \sqrt{\left(\frac{\partial u}{\partial z}\right)^2 + \left(\frac{\partial v}{\partial z}\right)^2 - \frac{g}{\rho_0}\frac{\partial \rho}{\partial z}} \le \nu^0_{T,S} .$$

In case of unstable stratification ($\partial\rho / \partial z \prec 0$), which may be appear during integration, the realization of this instability in the model was taken into account by increase of eddy diffusion coefficient 20 times in appropriate columns from the surface to the bottom.

4. Numerical method of solution

For the considered non-stationary, nonlinear problem existence (*Sukhonosov, 1981*) and uniqueness theorems of solution are proved (*Kordzadze, 1979,1982)*.

the two-cycle splitting method both on physical processes, and vertical coordinate planes and lines is used, which is described in detail in G.I. Marchuk's (1974) and A. A. Kordzadze’s monographies (1988).

After splitting of the model equation system on the physical processes following stages are allocated on each double time step $2\tau = t_{j+1} - t_{j-1}$:

1. The transfer of physical fields with taken into account eddy viscosity and diffusion on the time interval $t_j \le t \le t_{j-1}$

$$\begin{cases} \dfrac{\partial u_1}{\partial t} + \operatorname{div}\vec{u}^{\,j} u_1 = \dfrac{\partial}{\partial x}\mu\dfrac{\partial u_1}{\partial x} + \dfrac{\partial}{\partial y}\mu\dfrac{\partial u_1}{\partial y} + \dfrac{\partial}{\partial z}\nu\dfrac{\partial u_1}{\partial z}, \\ \dfrac{\partial v_1}{\partial t} + \operatorname{div}\vec{u}^{\,j} v_1 = \dfrac{\partial}{\partial x}\mu\dfrac{\partial v_1}{\partial x} + \dfrac{\partial}{\partial y}\mu\dfrac{\partial v_1}{\partial y} + \dfrac{\partial}{\partial z}\nu\dfrac{\partial v_1}{\partial z}, \\ \dfrac{\partial T_1}{\partial t} + \operatorname{div}\vec{u}^{\,j} T_1 = \dfrac{\partial}{\partial x}\mu_T\dfrac{\partial T_1}{\partial x} + \dfrac{\partial}{\partial y}\mu_T\dfrac{\partial T_1}{\partial y} + \dfrac{\partial}{\partial z}\nu_T\dfrac{\partial T_1}{\partial z} + \dfrac{\partial \nu_T\gamma_T}{\partial z}, \\ \dfrac{\partial S_1}{\partial t} + \operatorname{div}\vec{u}^{\,j} S_1 = \dfrac{\partial}{\partial x}\mu_S\dfrac{\partial S_1}{\partial x} + \dfrac{\partial}{\partial y}\mu_S\dfrac{\partial S_1}{\partial y} + \dfrac{\partial}{\partial z}\nu_S\dfrac{\partial S_1}{\partial z} + \dfrac{\partial \nu_S\gamma_S}{\partial z}. \end{cases} \tag{4.1}$$

2. The adaptation of the physical fields on the time interval $t_{j-1} \le t \le t_{j+1}$. There is solved following equation system:

$$\begin{aligned}
&\frac{\partial u_2}{\partial t} - l v_2 + \frac{1}{\bar{\rho}} \frac{\partial p_2}{\partial x} = 0,\\
&\frac{\partial v_2}{\partial t} + l u_2 + \frac{1}{\bar{\rho}} \frac{\partial p_2}{\partial y} = 0,\\
&\frac{\partial p_2}{\partial t} = g\left(\alpha_T T_2 + \alpha_S S_2\right),\\
&\frac{\partial u_2}{\partial x} + \frac{\partial v_2}{\partial y} + \frac{\partial w_2}{\partial z} = o,\\
&\frac{\partial T_2}{\partial t} + \gamma_T w_2 = 0,\\
&\frac{\partial S_2}{\partial t} + \gamma_S w_2 = 0.
\end{aligned} \qquad (4.2)$$

3. On the time interval $t_{j-1} \le t \le t_{j+1}$ the same transfer-diffusion equations (4.1) are solved for functions $u_3, v_3, w_3, p_3, T_3,$ and S_3 .

On each stage, equations are in turn split on coordinates. As a result, solution of nonstationary 3D problem is reduced to solution of a set of more simple problems.

Simulation of basin scale and regional annual mean Black Sea circulation

5.1 Some parameters and input data

The horizontal resolution of BSM was 5 km with grid points 225 along x axes and 111 –along y axes. The model has 32 calculated levels at depths:

1, 3, 5, 7, 11, 15, 25, 35, 55, 85, 135, 205, 305,…, 2205 m.

The dependence of albedo of the Black Sea surface upon zenithal angle was taken into account.
The parameter of absorption of solar radiation corresponded to usual ocean water, where about 10% of radiation reaches the depth of 10 km.

$g=980\ cm^2/s$, $\rho_0=1 g/cm^3$, $l_0=0{,}95.10^{-4}\ s^{-1}$, $\beta=10^{-13} cm^{-1}s^{-1}$, $\Delta t = 1h$, $c_T = c_S = 10$,

(a)

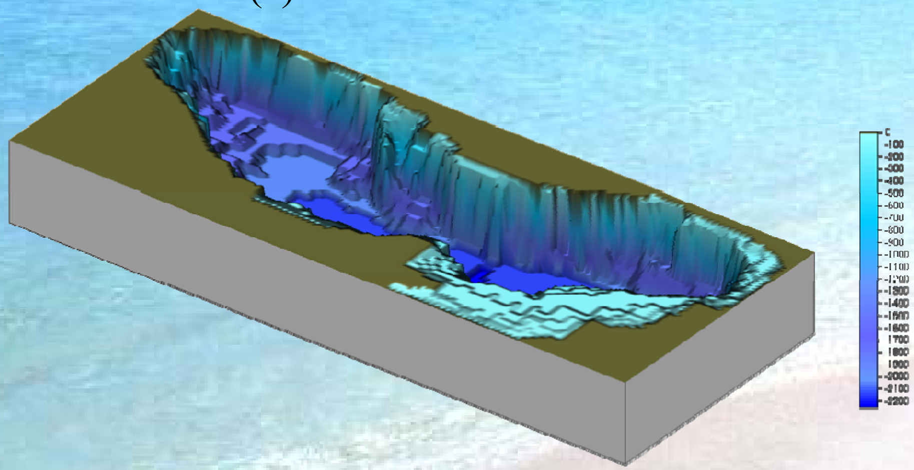

(b)

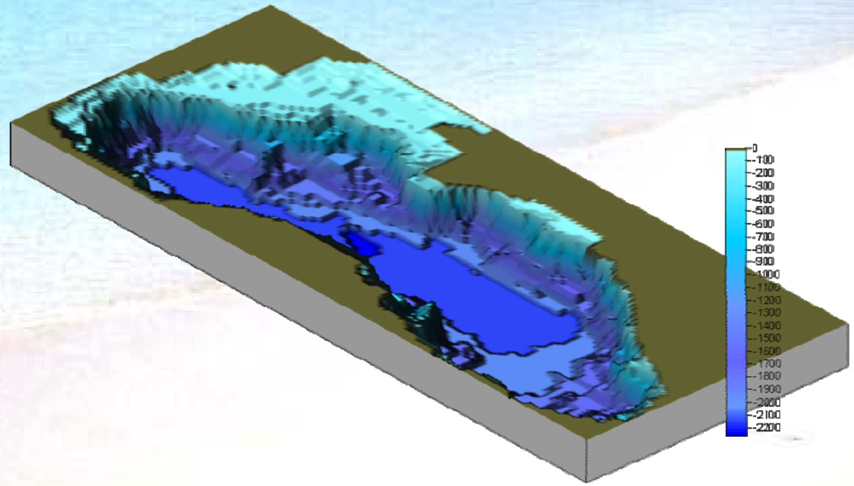

Fig.2. The spatial images of the Black Sea topography

(a) from northern and (b) southern sides.

We carried out numerical experiments on simulation of annual mean basin scale circulation. With the purpose of estimation of sensitivity of the model to the input data numerical experiments were carried out with the use of two kinds of climatic input data.

These data differed from each other in climatic fields of sea surface temperature and salinity and their profiles. The wind stress field was the same in both experiments.

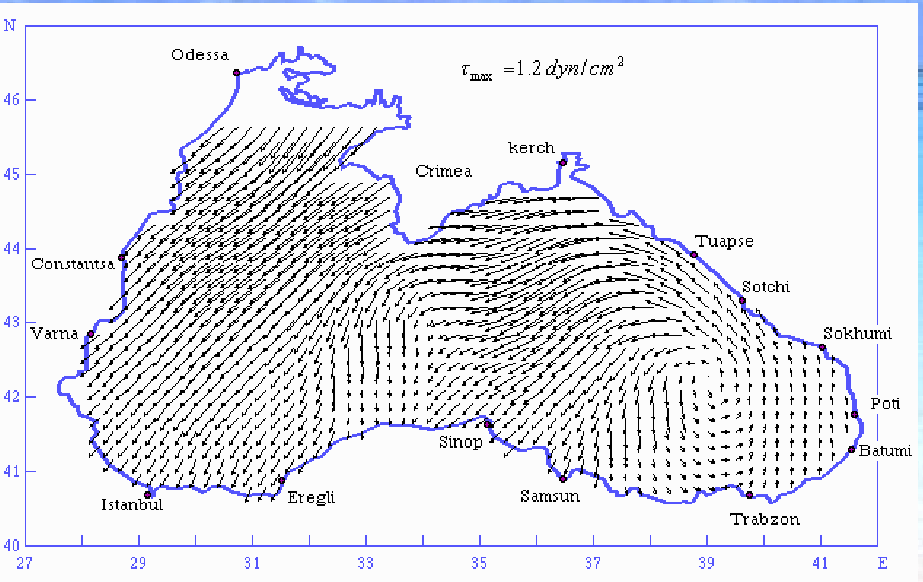

Fig.3 Annual mean climatic wind stress field used in numerical experiments

Temperature on z=0 | Salinity on z=0

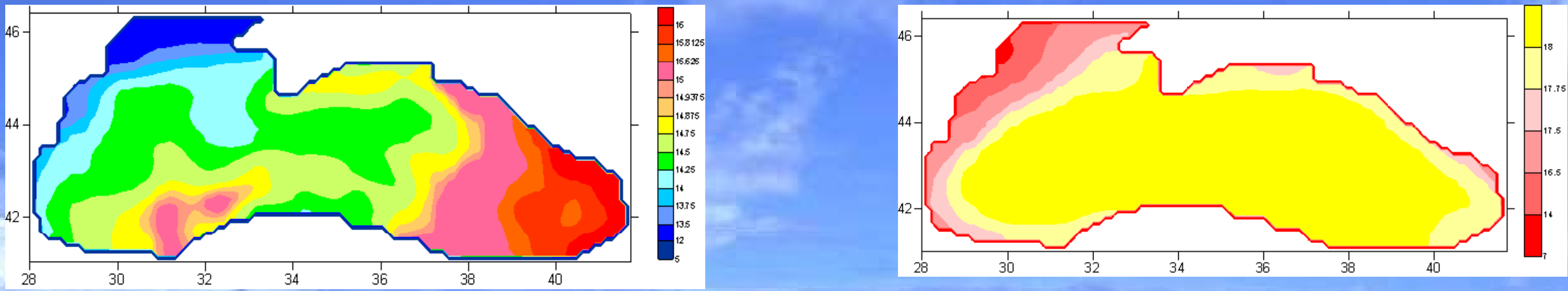

Fig.4 Annual mean climatic temperature and salinity fields on the sea surface (data A).

Temperature on z=0 | Salinity on z=0

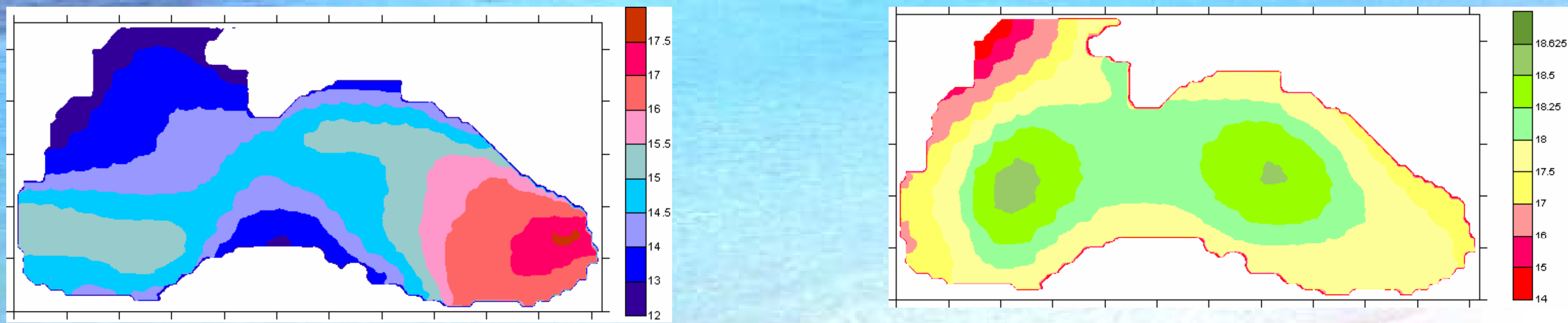

Fig.5 Annual mean climatic temperature and salinity fields on the sea surface (data B).

It is clear that more differences between data (A) and (B) are in salinity fields. Increase of salinity from periphery to the open part of the sea is more clearly expressed on the data (B), on a background of the general increase of salinity to the open part of the basin, areas of high salinity in the east and western parts of sea basin are observed.

Two numerical experiments on modeling an annual mean climatic state of the Black Sea were carried out. The equations of the model were integrated with zero initial conditions. Results of calculations were analyzed on the third modeling year at achievement of quasistationary state.

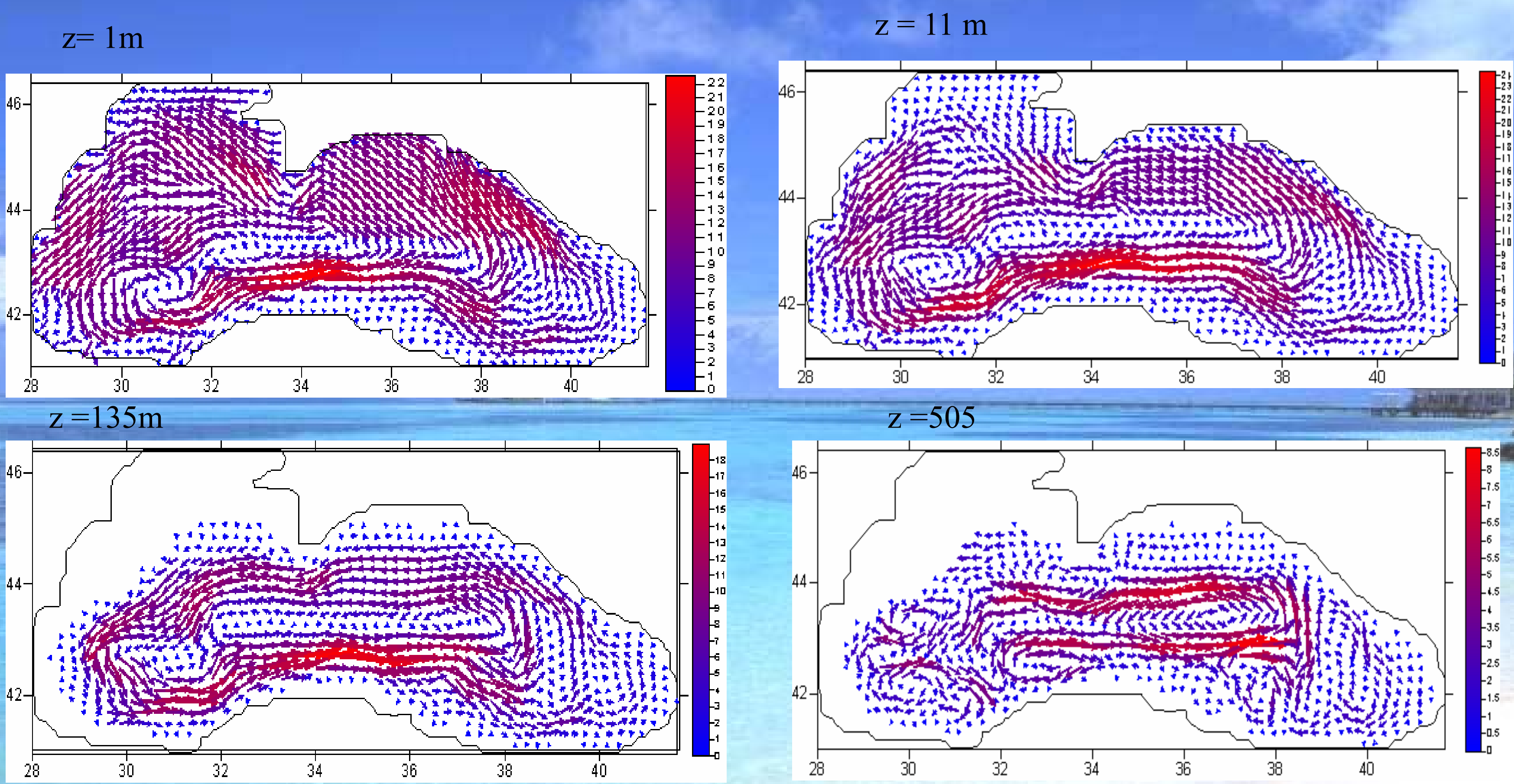

Fig.6 Modeling annual mean climatic current field on different depths (data A).

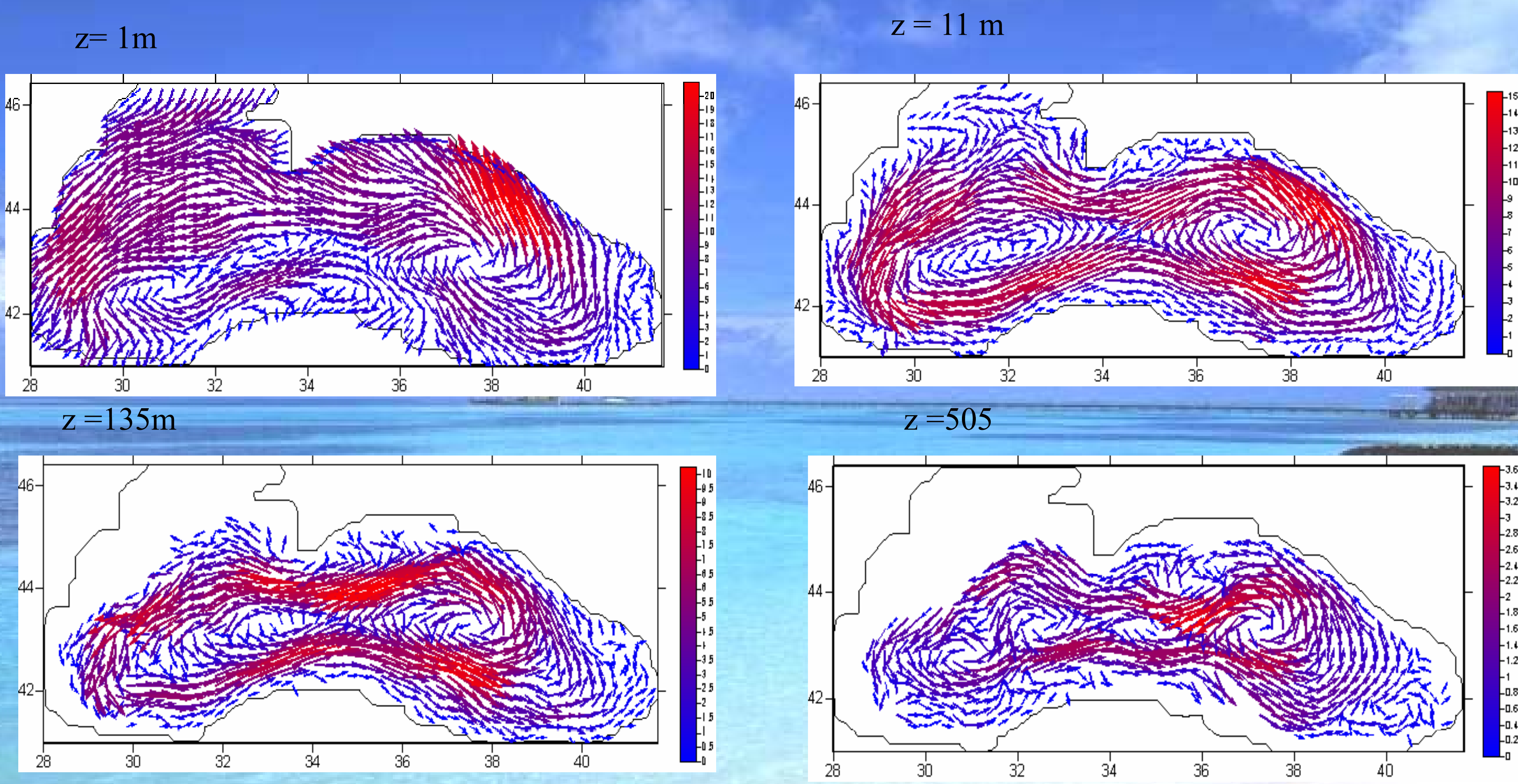

Fig.7. Modeling annual mean climatic current field on different depths (data B)

The comparison of results shows that in both cases the general cyclonic character of the Black Sea circulation is observed, which is kept in the deep layers with increase of vorticity of motion. Distinctive features of circulation are also obvious. By using the data (B) in the southeast part of the sea well expressed anticyclone (the Batumi anticyclone) is formed, which in this part of the sea is well-known from observations. Differences in structure of cyclonic eddies are observed as well. By using data (B) cyclonic eddies in the east

and western parts of the basin in the upper layer are more advanced and cover bigger territory. Among other distinctive features we note formation of the anticyclonic eddy on the east side of the
Crimean peninsula in the experiment using data (B). Finally, we can conclude that the results of the sea dynamics model significantly depend on input data. Therefore, providing high degree of data accuracy and applying assimilation methods are very importance for adequate reproduction of circulation processes.

Simulation of regional circulation processes.
Nested grid modeling.

For modelling of regional hydrodynamic processes in the east part of the Black Sea, calculated grid with a constant horizontal step equal to 1 km and quantity of points 216 and 347 on axes x and y respectively were used. In Fig. 8 the area of realization of a regional model with liquid boundary along E is represented. As boundary conditions on liquid boundary results of modeling of basin scale annual mean circulation were used (data (B)).

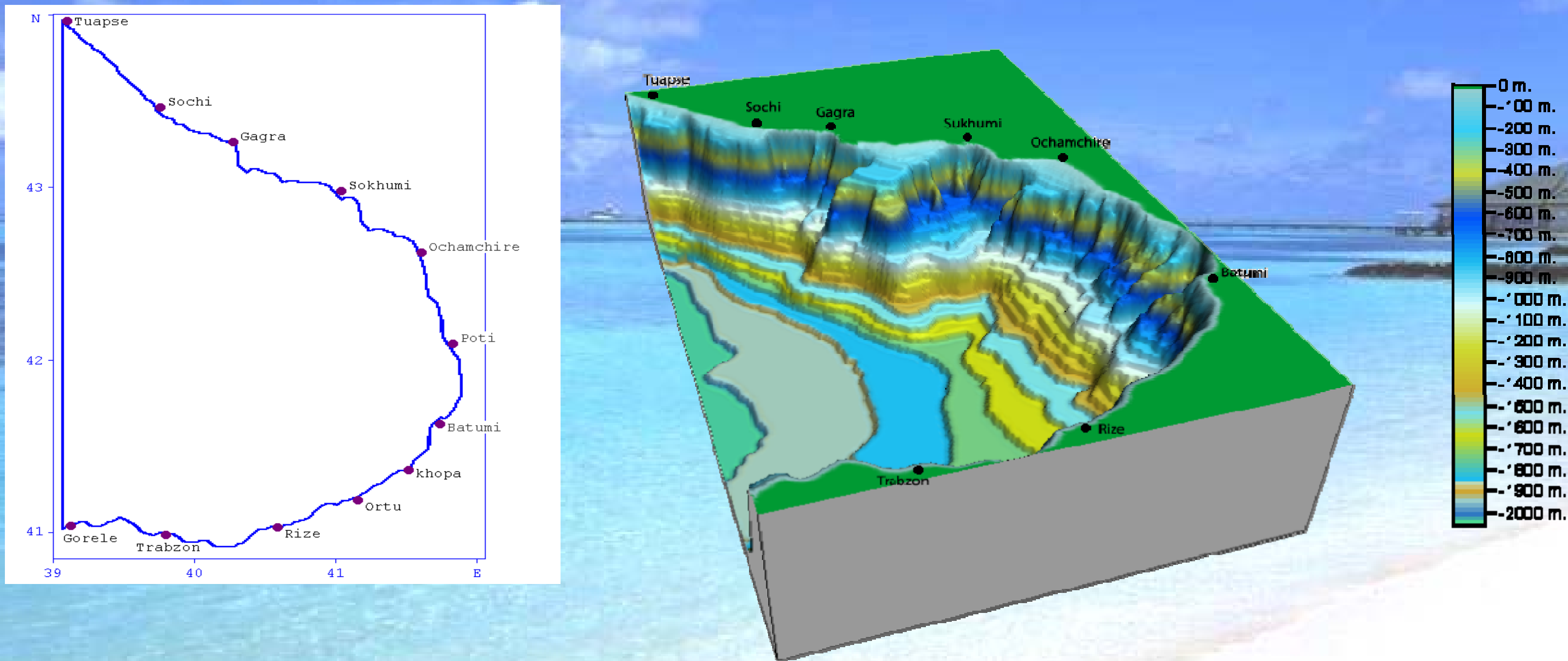

Fig.8. The area of solution and sea bottom topography in the east part of the Black Sea.

z = 1 m

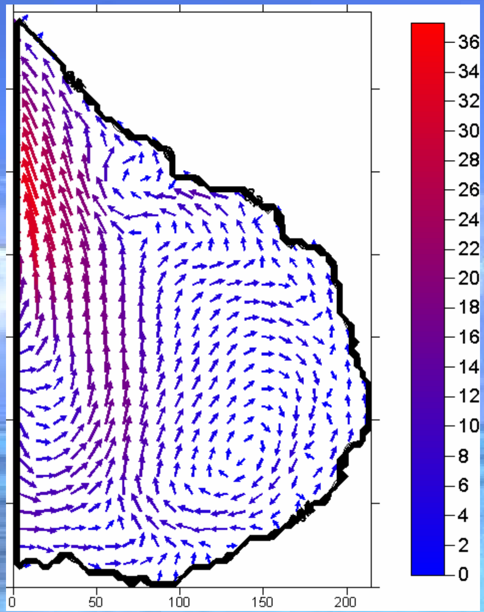

z = 55 m

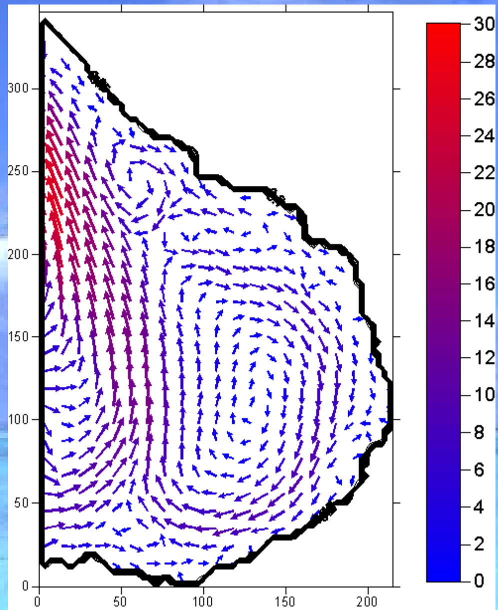

z = 305 m

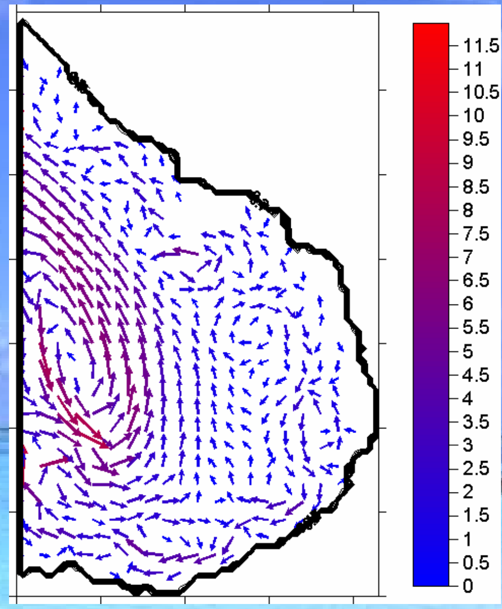

z = 505 m

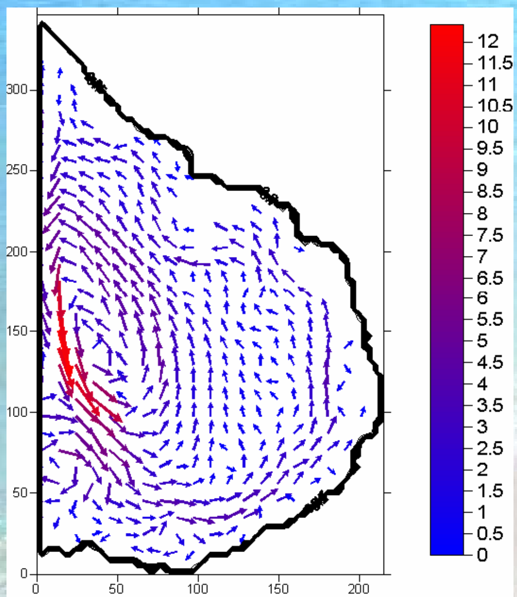

Fig.9. Annual mean circulation in the eastern coastal zone (liquid boundary is passing along meridian 39’05’) obtained by regional nested model.

In these Figures computed annual mean current field is shown on different depths. The model well describes coastal vortexes of small sizes which appear near Gagra and Sukhumi. Except these vortexes there is also more extensive anticyclonic vortex, which is similar to a well-known Batumi anticyclonic vortex.

Simulation of the nonstationary Black Sea circulation processes

One of the principal numerical experiments carried out on the basis of this model was simulation of inner-annual variability of the Black Sea hydrological regime in the conditions of alternation of different atmospheric wind types. These types were taken from ***Atlas of Excitement and Wind of the Black Sea*** (Leningrad, 1969), in which on the basis of processing observed data for 1946-1962 41 types of atmospheric circulation are established above territory of the Black Sea within one year. This experiment aimed at studying how the circulation system of the Black Sea responds to the variability of atmospheric processes.

Annual cycles of temperature and salinity at the sea surface and their vertical profiles, as well as the annual cycles of temperature, salinity, and water discharges at the open boundaries near the Danube River and the Bosporus reproduced on known monthly mean values with the use of a linear interpolation.

The beginning of integration corresponded to the 1st January and as initial conditions annual mean climatic model fields of current, salinity and temperature, calculated by the same model, were used (data A). Nonstationarity of atmospheric circulation was reduced to alternation of 24 wind types, that are characterized by the greatest repeatability over the Black Sea basin.

The numerical experiment has shown, that under influence of non-stationarity of atmospheric processes circulation in the upper layer of the Black Sea is characterized by significant qualitative and quantitative changes and within one year a continuous transformation of current system is possible to observe. The upper 20-30 m layer is especially sensitive to variability of the atmospheric forcing. Intensity of sea circulation was weakened in summer in process of easing atmospheric circulation and amplified in autumn and in winter when atmospheric winds became more intensive. So, for example, in summer in some periods of time in almost still conditions the current velocity decreased up to 10-12 cm/s, and in autumn and in winter achieved or slightly surpassed 100 cm/s in stormy winds. Such high current velocities are observed in the Black Sea (*Boguslavskij, Efimov et al, 1980; Stanev, Trukhchev et al, 1988*). Numerical simulation has also shown that intensive atmospheric circulation promotes disintegration of vortical formations in the upper layer and on the contrary - in case of weak winds vortex motion is well developed.

In order to illustrate the transformation of sea surface circulation during the winter period, we chose the time interval 622-744h (January; the time was counted from January 1), when atmospheric circulation was reorganized as shown in table.

№	Wind direction	Wind speed, m/s	Time intervals, hours
1	Northeasterly	1	622-636
2	Northerly	10-15	636-660
3	Northwesterly	1	660-674
4	Southwesterly	5-10	674-692
5	Westerly	1	692-706
6	Northwesterly	5-10	706-744

In Fig.10 wind stress fields on the sea surface corresponded to north-eastern and south-western type of winds are shown that were acted in the presented time interval.

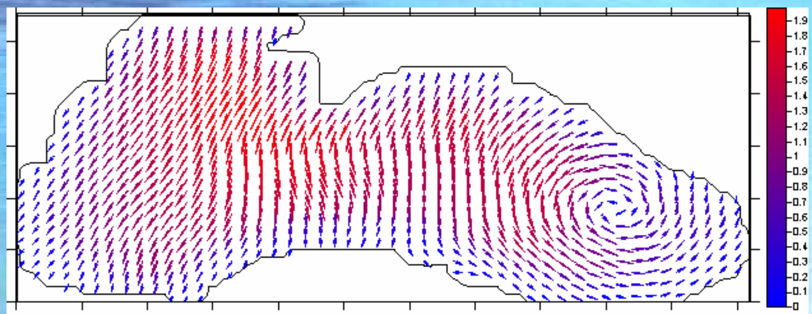

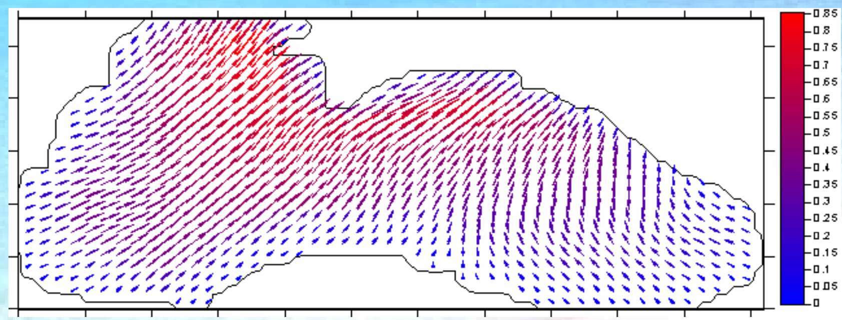

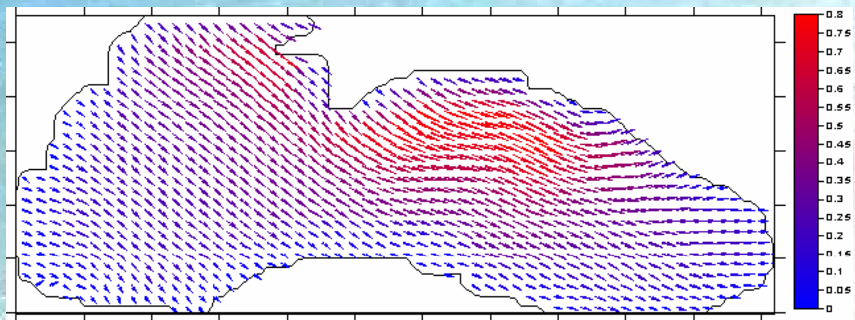

Fig.10. Wind stress fields corresponding to the northerly (10-15m/s) (a), southwesterly(5-10m/s) (б) and northwesterly winds.

Next Figures illustrate transformation of the Black Sea circulation on horizon z = 1m under influence of such atmospheric circulation.

t = 634 h

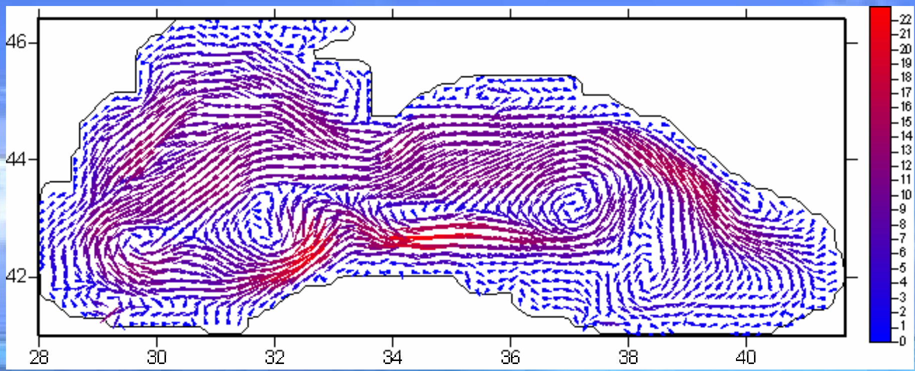

t = 658 h

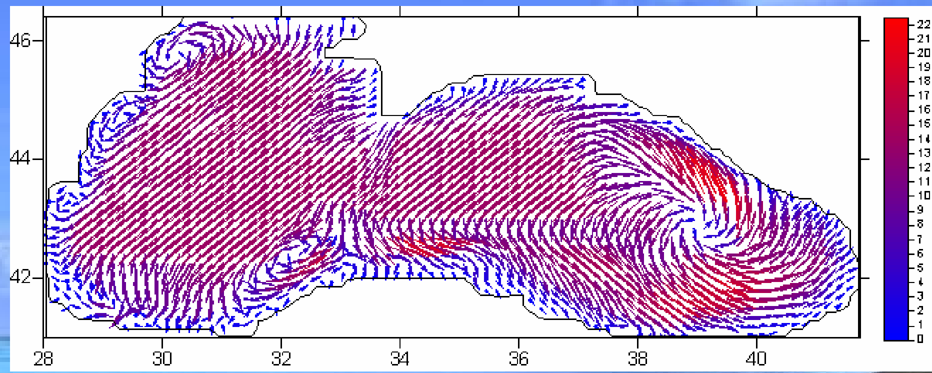

t = 672 h

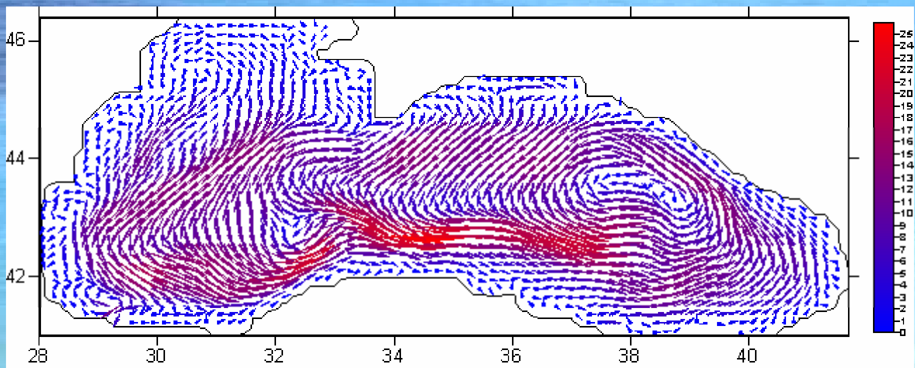

t = 690 h

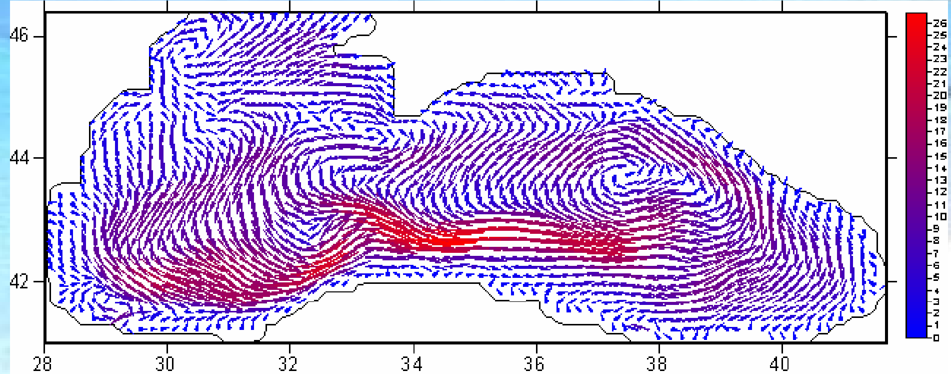

t = 704 h

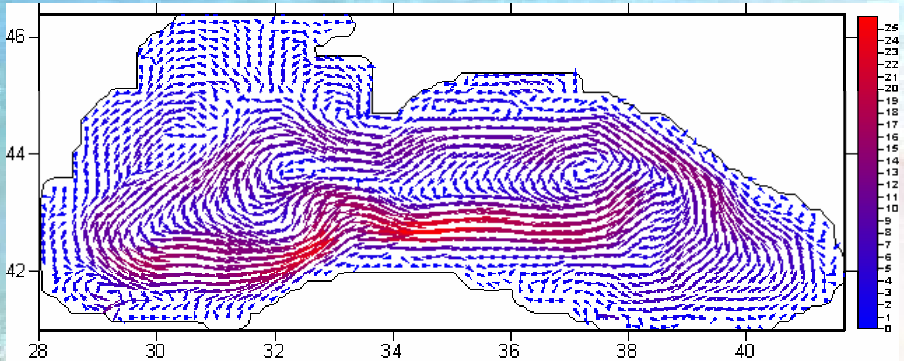

t = 742 h

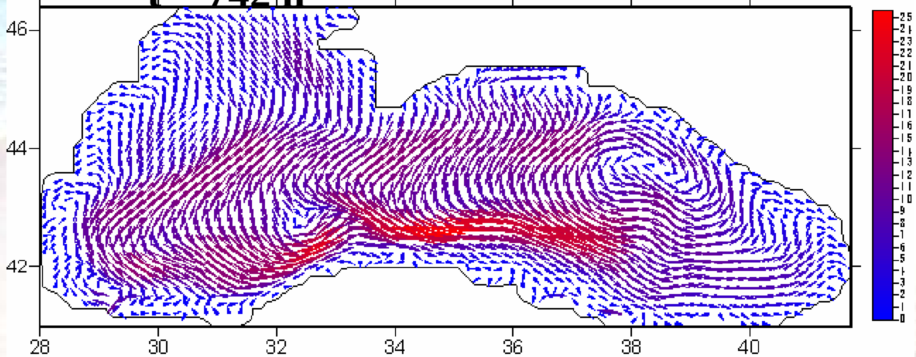

From these Figures it is visible, that vortex circulations is more well expressed in case of weak wind speeds.

Next Figures illustrate changeability of the surface temperature field in this numerical experiment. T changed insignificantly in such a short –term period. The same may be said about salinity field.

T E M P E R A T U R E

t = 634 h, z = 1m

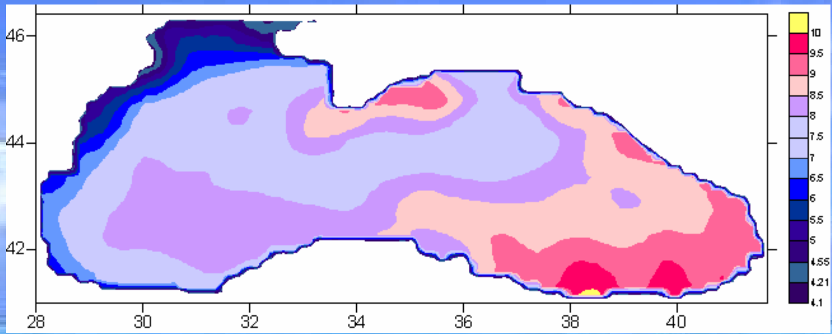

t = 658 h, z = 1m

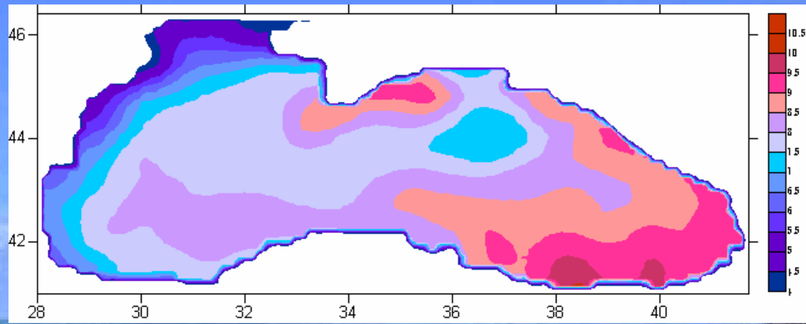

t = 672 h, z = 1m

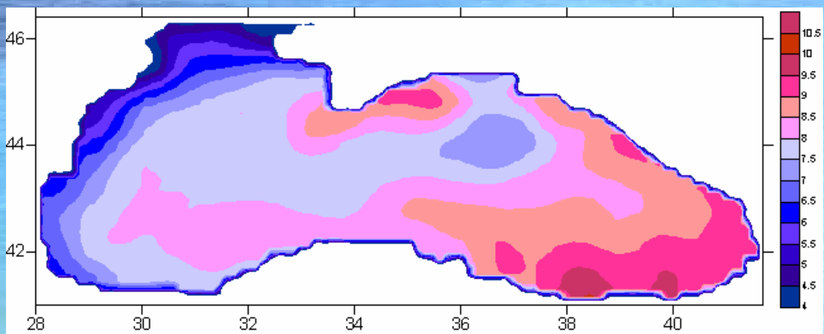

t = 690 h, z = 1m

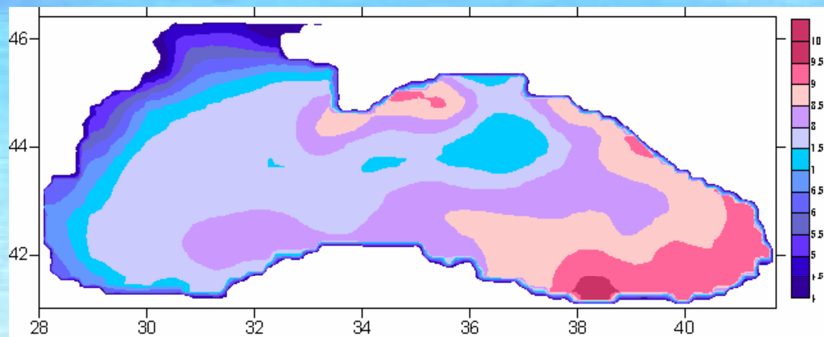

t = 704 h, z = 1m

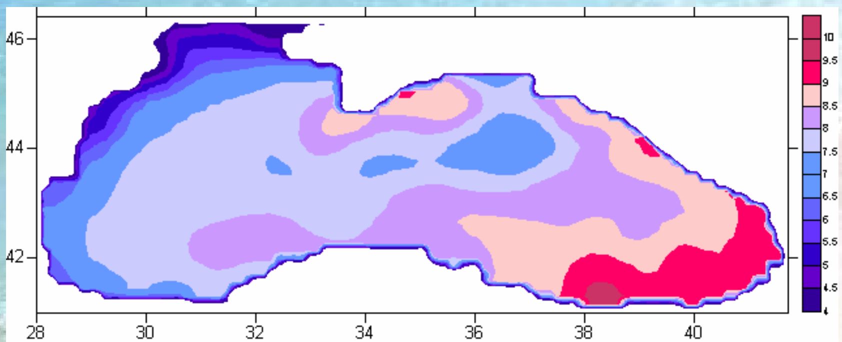

t = 742 h, z = 1m

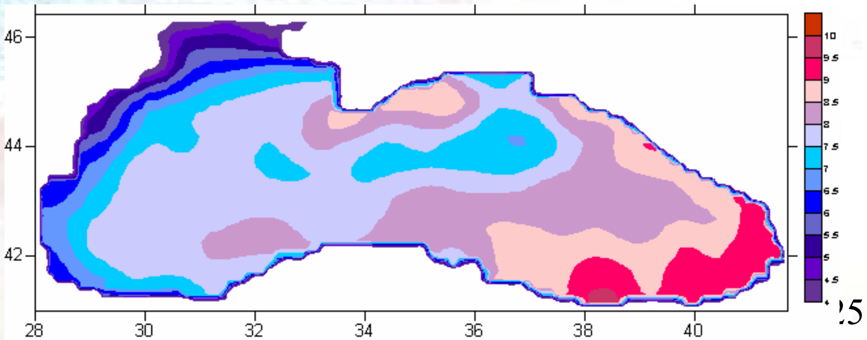

Next Figures illustrate the vertical structure of sea circulation in cases when the atmosphere state was close to calm and strong winds. During the moderate and strong winds, as the depth increases, the sea circulation experiences more substantial qualitative and quantitative changes than during weak winds.As a result from a depth of about 15-20m, the circulation acquires a vortical character.

t = 634h, z = 1m

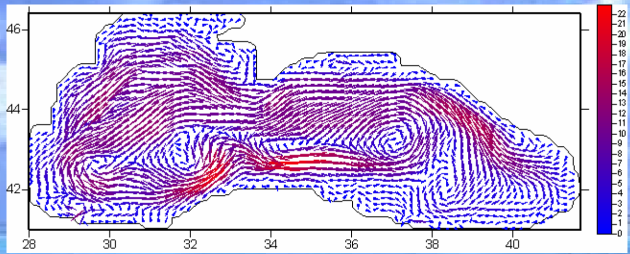

t = 658h, z = 1m

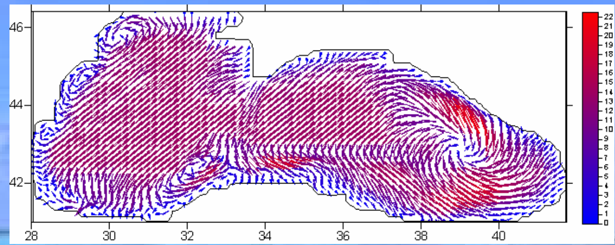

z = 11m

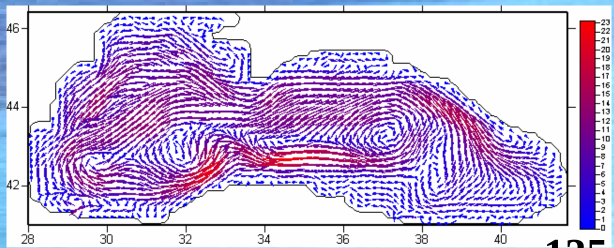

z = 11m

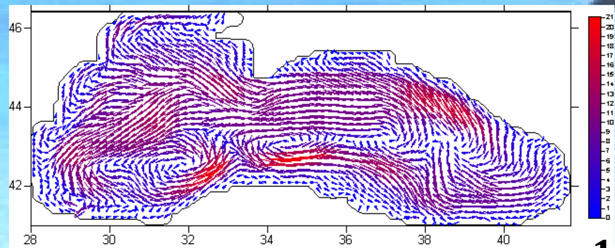

z = 135m

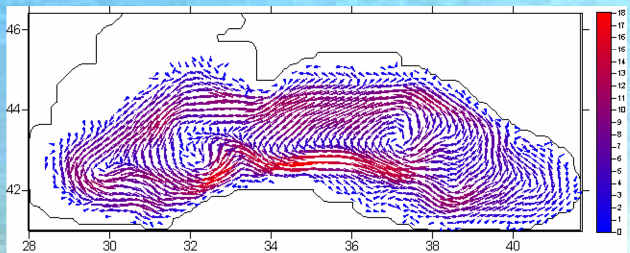

z = 135m

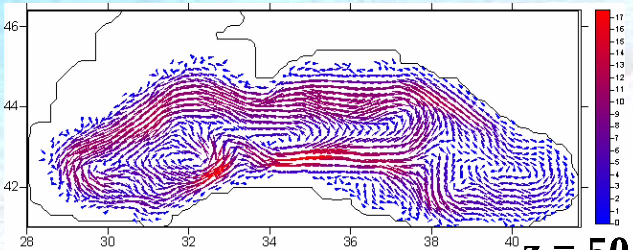

z = 505m

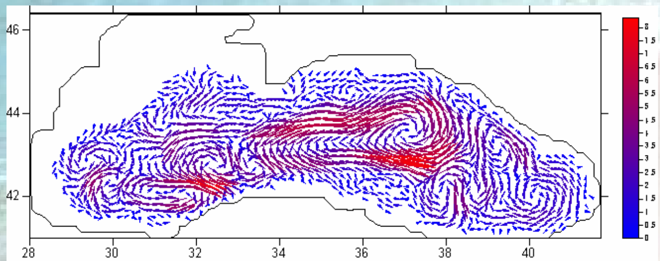

z = 505m

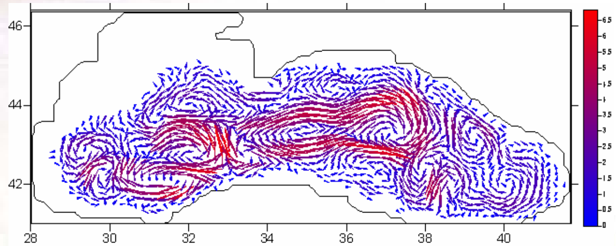

In order to illustrate the transformation of sea-surface circulation during the warm period we chose the time interval 2774 – 2862 h (the end of April), when the circulation was reorganized as shown in the table.

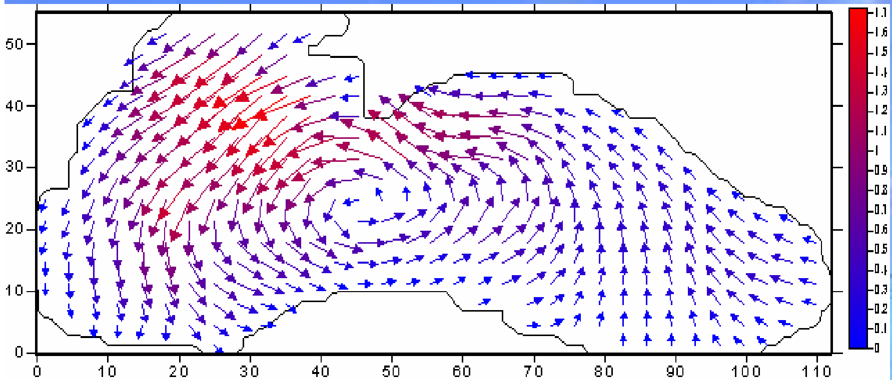

№	Wind direction	Wind speed, m/s	Time intervals, hours
1	**Cyclonic**	**5-10**	**2774-2798**
2	**Northwest.**	**1**	**2798-2822**
3	**Northwest.**	**10-15**	**2822-2838**
4	**Southwest.**	**1**	**2838-2862**

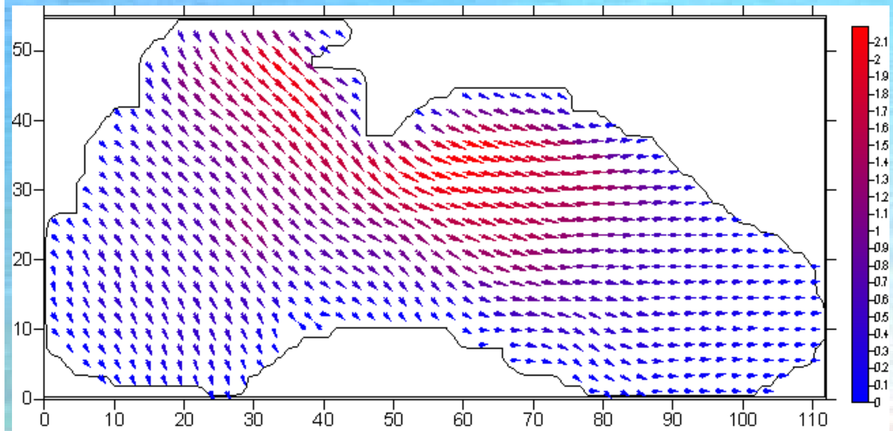

From these Figures it is visible, that vortex circulations is more well expressed in case of weak wind speeds. Among coastal anti-cyclonic eddies Batumi anticyclonic eddy in the southeast part of the basin is more intensive. Numerical experiment has shown that Batumi eddy is rather steady formation during warm season. It is interesting to note, that the similar conclusion is obtained by Korotaev, Oguz at al (2003).

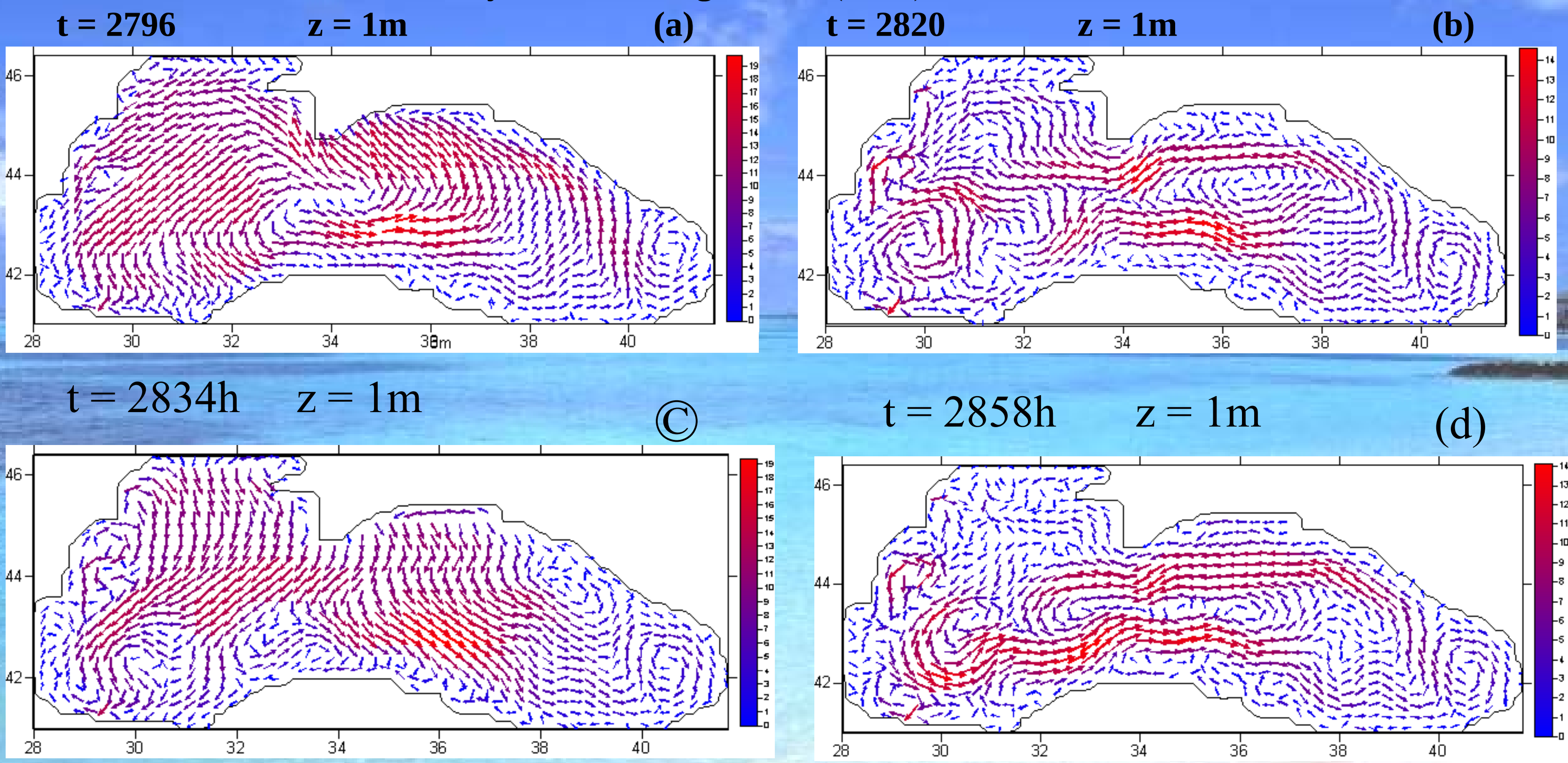

Fig.11. Current fields in April at depth of 1 m: (a) cyclonic wind (5-10 m/s), (b) calm (1m/s); (c) northerly wind (10-15 m/s); (d) calm (1m/s).


Thank You